Green's function Monte Carlo study of SU(3) lattice gauge theory in (3+1)D

C. J. Hamer,* M. Samaras, and R. J. Bursill†
School of Physics, University of New South Wales, Sydney, 2052, Australia
(Received 8 May 2000; published 8 September 2000)

A ''forward walking'' Green's function Monte Carlo algorithm is used to obtain expectation values for SU(3) lattice Yang-Mills theory in $3+1$ dimensions. The ground state energy and Wilson loops are calculated, and the finite-size scaling behavior is explored. Crude estimates of the string tension are derived, which agree with previous results at intermediate couplings, but more accurate results for larger loops will be required to establish scaling behavior at weak coupling.

PACS number(s): 11.15.Ha

I. INTRODUCTION

Classical Monte Carlo simulations provide a very powerful and accurate method for the study of Euclidean lattice gauge theories. In the Hamiltonian formulation [1], on the other hand, the corresponding quantum Monte Carlo methods have been somewhat neglected. Here we present a study of SU(3) Yang-Mills theory in $3+1$ dimensions, using the Green's function Monte Carlo approach [2], adapted to lattice gauge theory by Chin *et al.* [3].

Quantum Monte Carlo methods in Hamiltonian lattice gauge theory (LGT) have a somewhat checkered history. The first calculations used a strong-coupling basis involving discrete ''electric field'' link variables and a ''projector Monte Carlo'' approach [4,5], which used the Hamiltonian itself to project out the ground state. A later version of this was the ''stochastic truncation'' approach of Allton *et al.* [6]. Using this approach one can successfully compute string tensions and mass gaps for Abelian models [7]. For non-Abelian models, however, some technical problems arose [7]. The use of a Robson-Webber recoupling scheme [8] at the lattice vertices requires the use of Clebsch-Gordan coefficients or $6j$ symbols, which are not known to high order for SU(3); and furthermore, the ''minus sign'' problem rears its head, in that destructive interference occurs between different paths to the same final state. It may well be that a better choice of the strong-coupling basis, such as the ''loop representation,'' might avoid these problems, but this has not yet been demonstrated.

In the meantime, Heys and Stump [9] and Chin *et al.* [3] pioneered the use of ''Green's function Monte Carlo'' (GFMC) or ''diffusion Monte Carlo'' techniques in Hamiltonian LGT, in conjunction with a weak-coupling representation involving continuous gauge field link variables. This was successfully adapted to non-Abelian Yang-Mills theories [10–13], with no minus sign problem arising. In this representation, however, one is simulating the wave function in gauge field configuration space by a discrete ensemble or density of random walkers: it is not possible to determine the derivatives of the gauge fields for each configuration or to enforce Gauss's law explicitly, and the ensemble always relaxes back to the ground state sector. Hence one cannot compute the string tensions and mass gaps directly as Hamiltonian eigenvalues corresponding to ground states in different sectors, as one does in the strong-coupling representation. Instead, one is forced back to the more laborious approach used in Euclidean calculations: namely, to measure an appropriate correlation function, and estimate the mass gap as the inverse of the correlation length. We have introduced the ''forward-walking'' technique, well known in many-body theory [2,14–16], to measure the expectation values and correlation functions. The technique has been demonstrated for the cases of the transverse Ising model in $(1+1)$D [17] and the U(1) LGT in $(2+1)$D [18].

Here we apply the technique for the first time to a non-Abelian model, namely SU(3) Yang-Mills theory in $(3+1)$D. The ground state energy and Wilson loop values are calculated, and approximate values are extracted for the string tension in the weak-coupling regime. Comparisons are made with earlier calculations, where they are available [19].

Our conclusions are that the method is a viable one, but requires the use of an improved ''guiding wave function'' to achieve better accuracy. There are certain drawbacks intrinsic to the method [2,20], such as the necessity to use a branching algorithm and a guiding wave function, which tend to introduce substantial errors into the results, both statistical and systematic. For these reasons, it may be preferable to employ a path integral Monte Carlo approach to these models, which avoids the problems above.

Our methods are presented in Sec. II, the results are outlined in Sec. III, and our conclusions are discussed in Sec. IV.

II. METHOD

A. Lattice Hamiltonian

The Green's function Monte Carlo formalism has been adapted to SU(2) Yang-Mills theory by Chin, van Roosmalen, Umland and Koonin [11] and sketched for the SU(3) case by Chin, Long and Robson [13]. Here we provide a slightly fuller discussion of the SU(3) case, following the earlier treatment of Chin *et al.* [11].

The SU(3) lattice Hamiltonian is given by [13]

*Email address: cjh@newt.phys.unsw.edu.au
†Addresses: Department of Physics, UMIST, P.O. Box 88, Manchester, M60 1QD, UK and School of Physics, University of New South Wales, Sydney 2052, Australia.

$$H=\frac{g^2}{2a}\left\{\sum_l E_l^a E_l^a-\frac{\lambda}{3}\sum_p \mathrm{Tr}(U_p+U_p^\dagger)\right\} \tag{1}$$

where E_l^a is a component of the electric field at link l, $\lambda=6/g^4$, the index a runs over the 8 generators of SU(3), and U_p denotes the product of four link operators around an elementary plaquette.

The commutation relations between electric field and link operators are

$$[E_l^a,U_{l'}]=\frac{1}{2}\lambda^a U_l\delta_{ll'}, \tag{2}$$

choosing the E_l^a as left generators of SU(3), where the $\{\lambda^a,a=1,8\}$ are the Gell-Mann matrices for SU(3). We will work with the dimensionless operator

$$H=\frac{1}{2}\sum_l E_l^a E_l^a-\frac{\lambda}{6}\sum_p \mathrm{Tr}(U_p+U_p^\dagger). \tag{3}$$

The link variables are elements of the group SU(3) in the fundamental representation

$$U=\exp\left(-i\frac{1}{2}\lambda^a A^a\right). \tag{4}$$

There is no simple equivalent of the quaternion representation for SU(2). Following Beg and Ruegg [21], we can represent

$$U=\begin{pmatrix} z_1 & z_2 & z_3 \\ u_1 & u_2 & u_3 \\ w_1 & w_2 & w_3 \end{pmatrix} \tag{5}$$

where $\mathbf{z},\mathbf{u},\mathbf{w}$ are three-dimensional complex vectors; then if U is to be unitary, we require $\mathbf{z},\mathbf{u},\mathbf{w}$ to be orthonormal, and if U is to have determinant unity, we require

$$\epsilon_{ijk}z_i u_j w_k=1 \tag{6}$$

which is satisfied if

$$w_i=\epsilon_{ijk}z_i^* u_k^*. \tag{7}$$

One possible representation which satisfies these conditions is

$$\begin{aligned} z_1&=[1-i(x_3+x_8/\sqrt{3})]/N_1, \\ z_2&=(-x_2-ix_1)/N_1, \\ z_3&=(-x_5-ix_4)/N_1 \end{aligned} \tag{8}$$

where

$$N_1=[1+(x_3+x_8/\sqrt{3})^2+x_1^2+x_2^2+x_4^2+x_5^2]^{1/2} \tag{9}$$

and

$$u_3=(-x_7-ix_6)/N_2\equiv\tilde{u}_3/N_2, \tag{10}$$

$$u_2=[1-i(x_8/\sqrt{3}-x_3)]/N_1\equiv\tilde{u}_2/N_2, \tag{11}$$

$$u_1=\tilde{u}_1/n_2,\quad \tilde{u}_1=-[\tilde{u}_2 z_2^*+\tilde{u}_3 z_3^*]/z_1^* \tag{12}$$

where

$$N_2=[|\tilde{u}_1|^2+|\tilde{u}_2|^2+|\tilde{u}_3|^2]^{1/2} \tag{13}$$

and

$$w_i=\epsilon_{ijk}z_j^* u_k^*. \tag{14}$$

This involves 8 unrestricted parameters $\{x_a,a=1,\ldots,8\}$, as expected. For small $\mathbf{x}$,

$$U\approx I-i\lambda^a x^a, \tag{15}$$

i.e.

$$x^a\approx A^a/2, \tag{16}$$

where A^a is the gauge field on that link. The product of two link variables can be found by simple matrix multiplication.

B. Green's function Monte Carlo method

The Green's function Monte Carlo method employs the operator $\exp[-\tau(H-E)]$, i.e. the time evolution operator in imaginary time, as a *projector* onto the ground state $|\psi_0\rangle$:

$$|\psi_0\rangle\propto\lim_{\tau\to\infty}\{e^{-\tau(H-E)}|\Phi\rangle\}=\lim_{\Delta\tau\to0,N\Delta\tau\to\infty}e^{-N\Delta\tau(H-E)}|\Phi\rangle \tag{17}$$

where $|\Phi\rangle$ is any suitable trial state. To procure some variational guidance, one performs a ''similarity transformation'' with the trial wave function Φ, and evolves the *product* $\Phi|\psi_0\rangle$ in imaginary time. The heart of the procedure is the calculation of the matrix element corresponding to a single small time step $\Delta\tau$. Chin *et al.* [11] show that

$$\begin{aligned} &\langle\mathbf{x}'|\Phi e^{-\Delta\tau(H-E)}\Phi^{-1}|\mathbf{x}\rangle \\ &\quad=\prod_l\langle U_l'|N\left\{\exp\left(-\frac{1}{2}\Delta\tau E_l^a E_l^a\right)\right. \\ &\qquad\left.\times\exp[\Delta\tau E_l^a(E_l^a\ln\Phi)]\right\}|U_l\rangle \\ &\qquad\times\exp\{\Delta\tau[E-\Phi^{-1}H\Phi(\mathbf{x})]\}+O(\Delta\tau^2) \\ &\quad\equiv p(\mathbf{x}',\mathbf{x})w(\mathbf{x})+O(\Delta\tau^2) \end{aligned} \tag{18}$$

where $\mathbf{x}=\{U_l\}$ denotes an entire lattice configuration of link fields.

The product $\Phi|\psi\rangle$ is simulated by the density of an ensemble of random walkers, as in the SU(2) case. At the kth step, the ''weight'' of each walker at $\mathbf{x}_k$ is multiplied by $w(\mathbf{x}_k)$ and the next ensemble $\{\mathbf{x}_{k+1}\}$ is evolved from $\{\mathbf{x}_k\}$ according to the matrix element $p(\mathbf{x}_{\mathbf{k}+1},\mathbf{x}_\mathbf{k})$. The effect of

$p(\mathbf{x_{k+1}},\mathbf{x_k})$ is to alter each link variable U_l in $\{\mathbf{x_k}\}$ to U_l' by a Gaussian random walk plus a ''drift step'' guided by the trial wave function:

$$U' = \Delta U U_d U \tag{19}$$

where $U_d = \exp[i\frac{1}{2}\lambda^a (i\Delta\tau E^a \ln\Phi)]$ is the drift step, and ΔU is an SU(3) group element randomly chosen from a Gaussian distribution around the identity, with variance $\langle \Delta s^2\rangle = 8\Delta\tau$ (i.e. $\Delta\tau$ for each index a), where

$$\langle \Delta s^2\rangle \approx \sum_a A^a A^a = 8\Delta\tau \quad (\text{small } A^a) \tag{20}$$

or

$$\langle x^a x^a\rangle = \frac{1}{4}\langle A^a A^a\rangle \approx \frac{\Delta\tau}{4}, \quad \text{each } a. \tag{21}$$

The simulation is carried out for a large number of iterations $\Delta\tau$, until an equilibrium distribution $\Phi|\psi_0\rangle$ is reached. The energy E in Eq. (18) is adjusted after each iteration so as to maintain the total ensemble weight constant. The average value of E can then be taken as an estimate of E_0, the ground-state energy.

As time evolves, the weights of some walkers grow larger, while others grow smaller, which would produce an increased statistical error. To avoid this, a ''branching'' process is employed, whereby a walker with weight larger than some threshold is split into two independent walkers, while others with weights lower than another threshold are amalgamated. We use Runge's technique [22] for this purpose.

C. Trial wave function

The trial wave function is chosen to be the one-parameter form [13]

$$\Phi = \exp\left[\alpha \sum_p \mathrm{Tr}(U_p + U_p^\dagger)\right]. \tag{22}$$

Then the drift step is [11]

$$U_d = \exp\left[i\frac{\lambda^a}{2}(i\Delta\tau E^a \ln\Phi)\right] \equiv \exp\left[-i\frac{\lambda^a}{2}A_l^a\right] \tag{23}$$

for each link, where

$$A_l^a = -i\Delta\tau\frac{\alpha}{2}\sum_{p\in l}\mathrm{Tr}[\lambda^a U_l \ldots U_4^\dagger - \mathrm{H.c.}] \tag{24}$$

i.e.

$$x_l^a \approx \frac{A_l^a}{2} = -i\frac{\alpha\Delta\tau}{4}\sum_{p\in l}\mathrm{Tr}[\lambda^a U_l \cdots U_4^\dagger - \mathrm{H.c.}] \tag{25}$$

(note that the effect of E_l^a on a plaquette operator is to ''insert'' a $\lambda^a/2$ in front of the appropriate link operator U_l, to be followed by the remaining link operators in the plaquette, taken in the direction of the link l).

Finally, the trial energy factor is

$$\Phi^{-1}H\Phi = \sum_l \left\{\frac{\alpha^2}{8}\left(\sum_{p\in l}\mathrm{Tr}[\lambda^a U_l\cdots U_4^\dagger - \mathrm{H.c.}]\right)^2 + \left(\frac{2\alpha}{3} - \frac{\lambda}{24}\right)\sum_{p\in l}\mathrm{Tr}(U_p + U_p^\dagger)\right\}. \tag{26}$$

Therefore the weight factor is

$$\begin{aligned} w(\mathbf{x}) &= \exp\{\Delta\tau(E - \Phi^{-1}H\Phi)\} \\ &= \exp\left\{\Delta\tau\left[E_{trial} - \left(\frac{2\alpha}{3} - \frac{\lambda}{24}\right)\sum_l\sum_{p\in l} 2\,\mathrm{Re}\{\mathrm{Tr}\,U_p\}\right.\right. \\ &\quad \left.\left. + \frac{\alpha^2}{8}\sum_l\left(\sum_{p\in l} 2\,\mathrm{Im}\{\mathrm{Tr}[\lambda^a U_l\cdots U_4^\dagger]\}\right)^2\right]\right\}. \end{aligned} \tag{27}$$

D. Forward walking estimates

The ''forward walking'' technique is used to estimate expectation values [2]. Its application to the U(1) lattice gauge theory in $(2+1)$D was discussed by Hamer *et al.* [18]. It is based on the following equation: for an operator Q,

$$\begin{aligned} \langle Q\rangle_0 &= \frac{\langle\psi_0|Q|\psi_0\rangle}{\langle\psi_0|\psi_0\rangle} \\ &\underset{J\to\infty}{\sim} \frac{\langle\Phi\,|K^J Q|\psi_0\rangle}{\langle\Phi|K^J|\psi_0\rangle} \\ &= \frac{\sum \tilde{K}(\mathbf{x}_J,\mathbf{x}_{J-1})\cdots\tilde{K}(\mathbf{x}_2,\mathbf{x}_1)Q(\mathbf{x}_1)\tilde{\psi}_0(\mathbf{x}_1)}{\sum \tilde{K}(\mathbf{x}_J,\mathbf{x}_{J-1})\cdots\tilde{K}(\mathbf{x}_2,\mathbf{x}_1)\tilde{\psi}_0(\mathbf{x}_1)} \end{aligned} \tag{28}$$

where $K(\mathbf{x}_J,\mathbf{x}_{J-1})$ is the evolution operator for time $\Delta\tau$, and $\tilde{K}(\mathbf{x}_J,\mathbf{x}_{J-1})$ is the same operator in the similarity transformed basis. Again we have assumed that the operator Q is diagonal in the basis of plaquette variables $\mathbf{x}$.

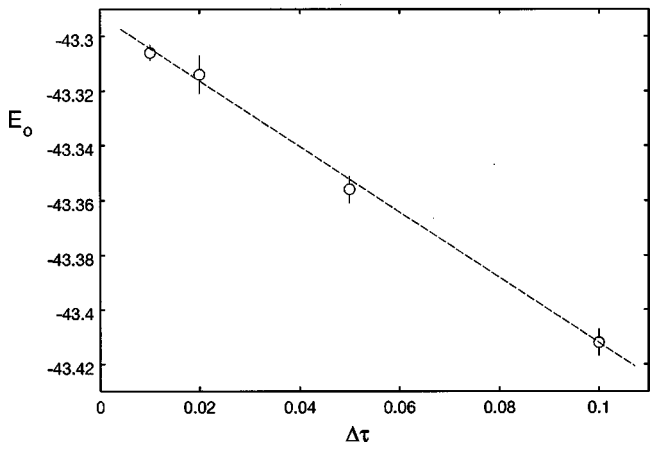

FIG. 1. Estimated ground-state energy for lattice size $L=4$ and coupling $\lambda=3.0$, $c=0.20$, as a function of time step $\Delta\tau$.

TABLE I. Variational parameter c, ground state energy per site ϵ_0 and Wilson loops $W(n,m)$ as functions of the lattice size L and coupling λ.

λ	1.5	3.0	4.0	5.0	6.0	9.0
c	0.10	0.20	0.27	0.33	0.40	0.58
Ground state energy per site, ϵ_0						
$L=2$	−0.15449(2)	−0.68081(1)	−1.3212(5)	−2.359(1)	−3.666(2)	−8.389(6)
3	−0.15438(4)	−0/6764(2)	−1.2846(3)	−2.187(1)	−3.431(2)	−8.042(4)
4	−0.15436(1)	−0.6764(1)	−1.2836(8)	−2.160(3)	−3.322(4)	−7.94(1)
6	−0.15436(2)	−0.6765(1)	−1.2809(7)	−2.133(2)	−3.234(3)	−7.613(9)
8	-	−0.6759(2)	−1.2705(4)	−2.094(2)	−3.154(2)	−7.402(6)
Wilson loops, $W(1,1)$						
$L=2$	0.0721(2)	0.1671(3)	0.273(2)	0.396(6)	0.460(7)	0.576(4)
3	0.0718(2)	0.1641(4)	0.245(2)	0.346(4)	0.437(5)	0.562(2)
4	0.0718(2)	0.1647(7)	0.240(2)	0.330(4)	0.401(5)	0.556(4)
6	0.0718(1)	0.1648(4)	0.240(3)	0.310(1)	0.383(2)	0.550(3)
8	-	0.1633(8)	0.228(1)	0.296(1)	0.365(2)	0.545(2)
$W(2,1)$						
3	0.0059(1)	0.0318(3)	0.070(1)	0.146(4)	0.234(6)	0.376(3)
4	0.0061(1)	0.0322(4)	0.067(2)	0.130(4)	0.182(4)	0.355(6)
6	0.0061(1)	0.0322(3)	0.069(2)	0.109(1)	0.165(2)	0.329(3)
8	-	0.0309(5)	0.057(1)	0.097(1)	0.144(2)	0.313(2)
$W(2,2)$						
4	-	0.0010(7)	0.006(2)	0.022(5)	0.044(5)	0.183(7)
6	-	0.0022(3)	0.009(2)	0.018(1)	0.037(2)	0.137(4)
8	-	0.0011(6)	0.005(1)	0.013(1)	0.023(2)	0.111(3)
$W(3,2)$						
6	-	-	-	0.004(1)	0.006(2)	0.059(3)
8	-	-	-	0.001(1)	0.004(1)	0.039(2)
$W(3,3)$						
6	-	-	-	-	-	0.020(3)
8	-	-	-	-	-	0.009(2)

This equation is implemented by [14–16] the following procedure:

(i) Record the value $Q(\mathbf{x}_i)$ for each ''ancestor'' walker at the beginning of a measurement.

(ii) Propagate the ensemble as normal for J iterations, keeping a record of the ''ancestor'' of each walker in the current population.

(iii) Take the weighted average of the $Q(\mathbf{x}_i)$ with respect to the weights of the descendants of $\mathbf{x}_i$ after the J iterations, using sufficient iterations J that the estimate reaches a ''plateau.''

III. RESULTS

Simulations were carried out for $L\times L\times L$ lattices up to $L=8$ sites, using runs of typically 4000 iterations and an ensemble size of 250–1000 depending (inversely) on lattice size. These statistics are approximately 100 times less than those used in the U(1) calculations [18], but about 100 times greater than those used in the previous SU(3) calculations of Chin *et al.* [13]. Time steps $\Delta\tau$ of 0.01 and 0.05 ''sec'' were used, with each iteration consisting of 5 sweeps and 1 sweep through the lattice, respectively, followed by a branching process. The first 400 iterations were discarded to allow for equilibration. The data were block averaged over blocks of up to 256 iterations, to minimize the effect of correlations on the error estimates.

The results taken at $\Delta\tau=0.01$ and $\Delta\tau=0.05$ were extrapolated linearly to $\Delta\tau=0$. Figure 1 demonstrates that the dependence of the ground-state energy on $\Delta\tau$ is approximately linear.

The variational parameter c was given values as shown in Table I. These are essentially the values used by Chin *et al.* [13], obtained from a variational Monte Carlo calculation. We checked that these were approximately the optimum values for small lattices.

Forward-walking measurements were taken over J iterations, where J ranged from 20 to 100, depending on the coupling λ. Ten separate measurements were taken over this time interval, in order to check whether the value measured by forward walking had reached equilibrium. A new measurement was started soon after the previous one had finished.

A. Ground-state energy

The dependence of the ground-state energy on the variational parameter c is illustrated in Fig. 2. It can be seen that

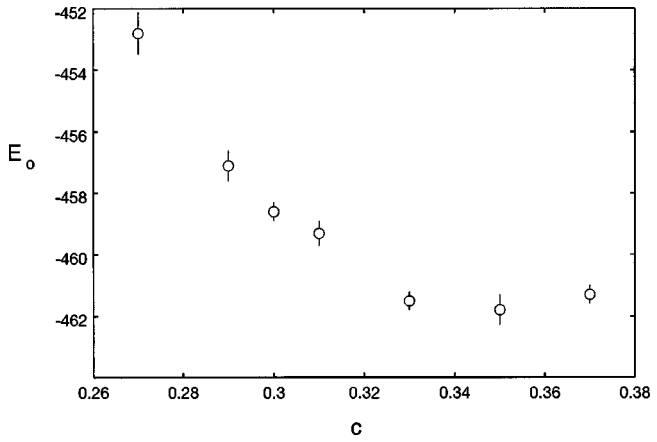

FIG. 2. Estimated ground-state energy as a function of the variational parameter c, for $L=6,\lambda=5.0$.

the energy reaches a broad minimum at about the expected value ($c=0.33$ at this coupling).

Our estimates of the ground-state energy are listed in Table I as a function of the coupling λ and lattice size L. The dependence on lattice size is illustrated in Fig. 3, at two fixed couplings $\lambda=3.0$ and $\lambda=5.0$. In the ''strong-coupling'' case, $\lambda=3.0$, it can be seen that the results converge exponentially fast in L, whereas in the ''weak-coupling'' regime, $\lambda=5.0$, the convergence is more like $1/L^4$ at these lattice sizes. This behavior merits some further explanation.

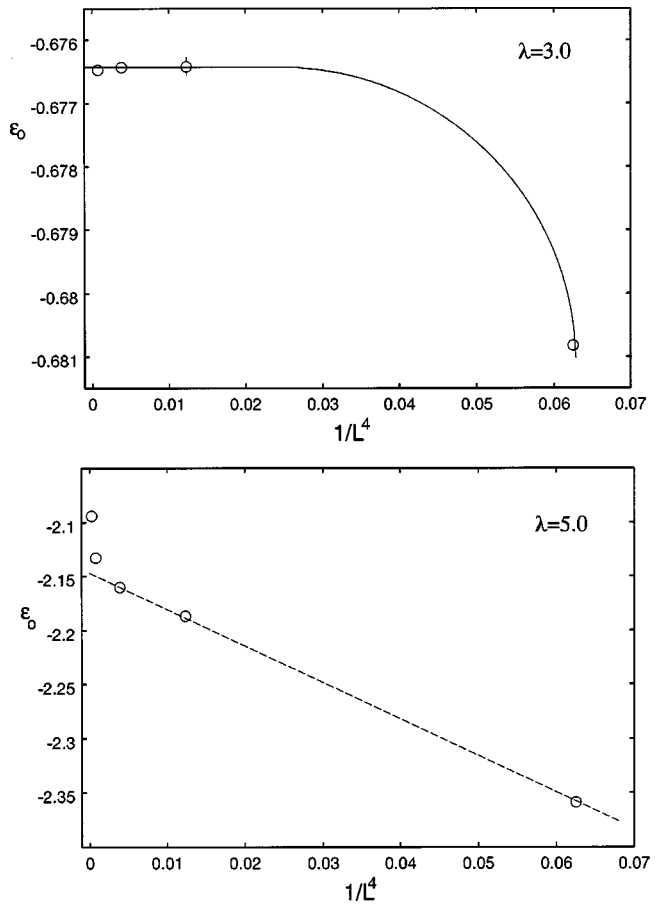

FIG. 3. Ground-state energy per site graphed against $1/L^4$, where L is the lattice size (a) at coupling $\lambda=3.0$, (b) at coupling $\lambda=5.0$. The lines are merely to guide the eye.

A similar phenomenon occurs in the case of the U(1) theory in $(2+1)$D [23,7,18]. In the strong-coupling regime, where the mass gap is large, the usual exponential convergence occurs. In the weak-coupling regime, however, where the mass gap M is very small, the finite-size scaling behavior for small lattice sizes is that of a massless theory, and it is only at much larger lattice sizes $L\approx 1/M$ that a crossover to exponential convergence occurs. In the U(1) case, it has been shown [7,18] that the finite-size scaling behavior at small L is well described by an ''effective Lagrangian'' approach, using the Lagrangian for free, massless photons that the model was originally constructed to simulate. In the same way, an ''effective Lagrangian'' corresponding to free, massless gluons (non-interacting QCD) should describe the finite-size behavior in the present case, in line with the idea of asymptotic freedom. By analogy with the $(2+1)$D case, we expect a $1/L^4$ dependence for the corrections to the ground-state energy per site. We hope to pursue this analysis further at a later date.

An anomalous feature in Fig. 3(b) is that the $L=8$ point lies well out of line with the others. This occurs at other couplings also. We suspect that the results for $L=8$ are not reliable, and that the trial wave function will have to be further improved to give reliable results for such large lattices. Supporting evidence for this will be presented below.

We have made estimates of the bulk limit, extrapolating mainly from the smaller L values where possible, and the results are listed in Table II. Our present estimates generally lie a little below those of Chin *et al.* [13], and we believe them to be more accurate in view of our greater statistics. The estimates for the bulk ground-state energy per site are graphed as a function of coupling in Fig. 4, where they are compared with previous estimates [19] obtained by an ''exact linked cluster expansion'' (ELCE) procedure and with the asymptotic weak-coupling series [24]

$$\epsilon_0 \sim -3\lambda + 7.798\lambda^{1/2}, \quad \lambda \to \infty. \tag{29}$$

The Monte Carlo results agree very well with the ELCE estimates, and appear to match nicely the expected weak-coupling behavior for $\lambda \geqslant 6$.

B. Wilson loops

The forward-walking method was used to estimate values for the $m\times n$ Wilson loops, $W(m,n)$. Figure 5 shows an example, namely the estimate of the mean plaquette $W(1,1)$ as a function of J for the case $L=6$, $\lambda=1.5$. It can be seen that the estimate relaxes exponentially towards a plateau value as the number of iterations, J, increases: an exponential fit is performed to estimate the asymptotic value. It can also be seen that the statistical error in each point is much larger than the point-to-point variation: the estimates are highly correlated, and all the points tend to move up and down together as one goes from one sample to the next.

A problem that arises in these measurements is the loss of statistical accuracy at large couplings. At large couplings the

TABLE II. Estimates of the bulk ground-state energy per site and Wilson loops as functions of λ.

λ	1.5	3.0	4.0	5.0	6.0	9.0
Ground state energy per site, ϵ_0						
This work	−0.15436(2)	−0.6764(1)	−1.284(2)	−2.16(2)	−3.25(2)	−7.9(1)
Chin *et al.* [13]		−0.675(0)	−1.275(3)	−2.088(6)	−3.183(6)	−7.50(3)
Wilson loops $W(1,1)$						
This work	0.0718(2)	0.165(1)	0.240(1)	0.32(1)	0.39(1)	0.554(3)
Chin *et al.* [13]		0.1605(5)		0.298(5)	0.377(3)	0.539(3)
$W(2,1)$						
This work	0.0061(2)	0.0322(5)	0.068(2)	0.12(1)	0.165(5)	0.34(1)
$W(2,2)$						
This work		0.0021(1)	0.008(4)	0.018(4)	0.035(7)	0.13(1)
$W(3,2)$						
This work				0.004(2)	0.006(2)	0.05(1)
$W(3,3)$						
This work						0.01(1)

weights of the random walkers vary rapidly with time, and it can easily happen that during a measurement the descendants of all the ''ancestor'' walkers but one die out from the ensemble, at which point the result ''freezes,'' and the number of members of the ensemble has effectively been reduced to 1. This inevitably means a severe loss of statistical accuracy.

A graph of the ''mean plaquette'' $W(1,1)$ versus the variational parameter c is shown in Fig. 6. Another problem is immediately apparent. The estimate for $W(1,1)$ is not independent of c—in fact it depends linearly on c over this range—and the size of the variation is such that the probable systematic error due to the choice of c is an order of magnitude larger than the random statistical error in the results. Thus it would be advatageous in future studies to put more effort into improving the trial wave function, rather than merely improving the statistics.

Figure 7 shows examples of the dependence of the results on lattice size L. Once again, the results at strong coupling $\lambda = 1.5$ converge exponentially fast, while those at the weak coupling value $\lambda = 5.0$ can be approximately fitted by a $1/L^4$ dependence. The $L=8$ value and even the $L=6$ value again lie off the trend of the smaller lattices, and are probably not very reliable.

Estimates of the bulk limit are listed in Table II. The estimates for the mean plaquette are graphed as a function of coupling λ in Fig. 8, and compared with series estimates at strong and weak coupling [19,24]. The agreement is quite good.

C. String tension

Having obtained estimates for the Wilson loop values on the bulk lattice, one can extract estimates for the ''spacelike'' string tension using the Creutz ratios

$$Ka^2 \simeq R_n = -\ln\left[\frac{W(n,n)W(n-1,n-1)}{W(n,n-1)^2}\right] \tag{30}$$

or the cruder 2-point estimates

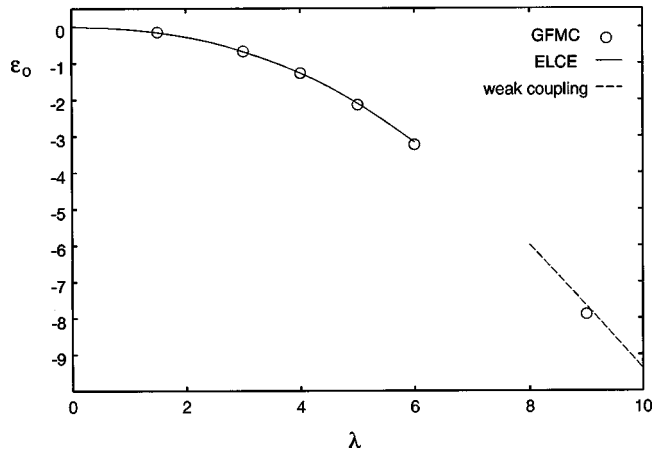

FIG. 4. The bulk ground-state energy per site graphed against coupling λ. The points are our Monte Carlo estimates, the solid line represents earlier ELCE estimates [19], and the dashed line represents the asymptotic weak-coupling behavior.

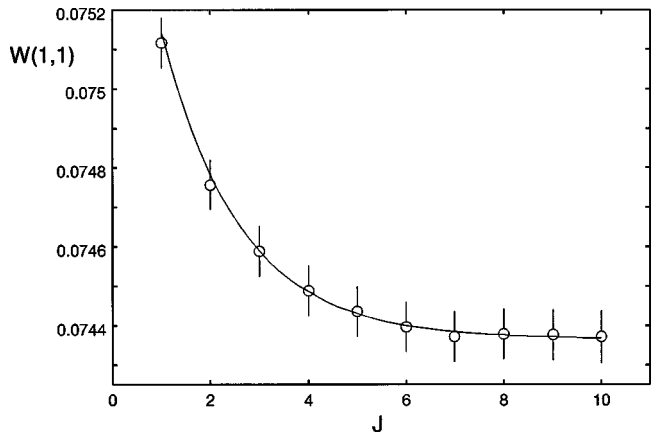

FIG. 5. Measured value for the Wilson loop $W(1,1)$ as a function of the number of forward-walking iterations, J, for the case $L=6$, $\lambda = 1.5$. The solid line is an exponential fit to the data.

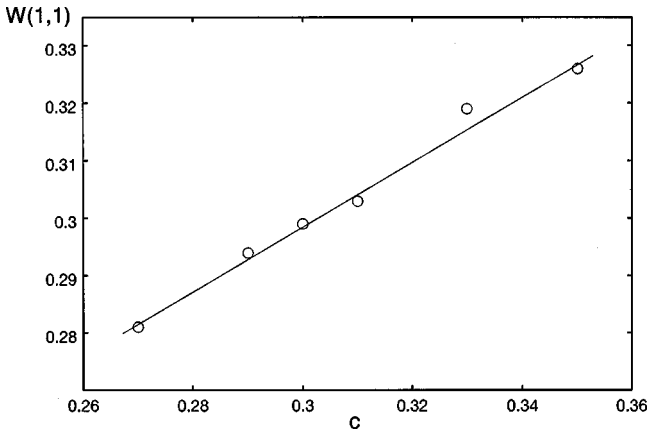

FIG. 6. Estimated value for the mean plaquette $W(1,1)$ as a function of the variational parameter c, for $L=6$, $\lambda=5.0$.

$$R_n' = -\frac{1}{n}\ln\left[\frac{W(n,n)}{W(n,n-1)}\right]. \tag{31}$$

The results are shown in Fig. 9. Also shown in Fig. 9 are some previous estimates derived from the ''axial'' string tension, obtained [19] using an ELCE method. The axial string tension aT is calculated as an energy per link, and must be converted to a dimensionless, ''spacelike'' tension by dividing by the ''speed of light'' c,

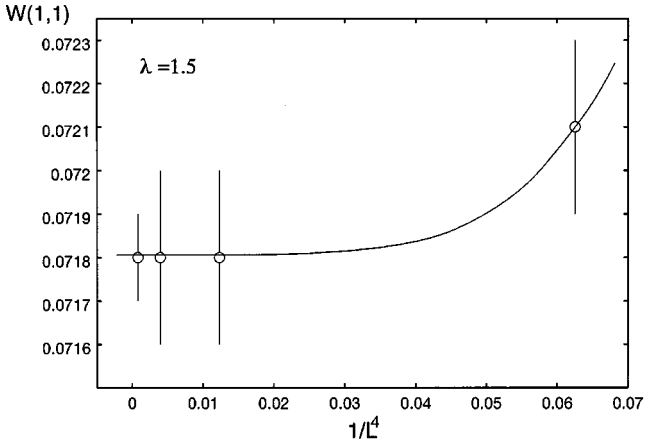

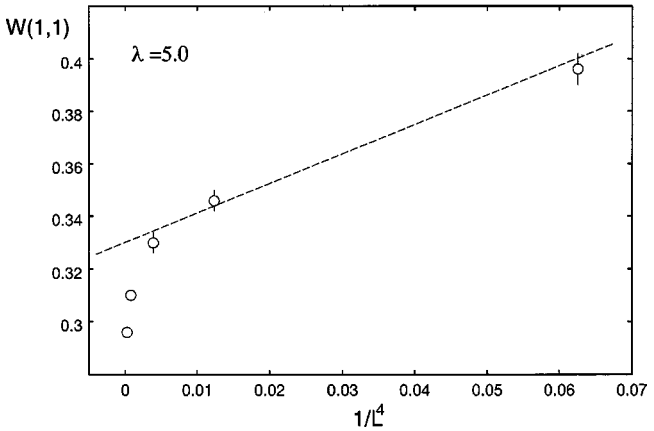

FIG. 7. The mean plaquette $W(1,1)$ graphed against $1/L^4$, where L is the lattice size (a) at coupling $\lambda=1.5$, (b) at coupling $\lambda=5.0$. The lines are merely to guide the eye.

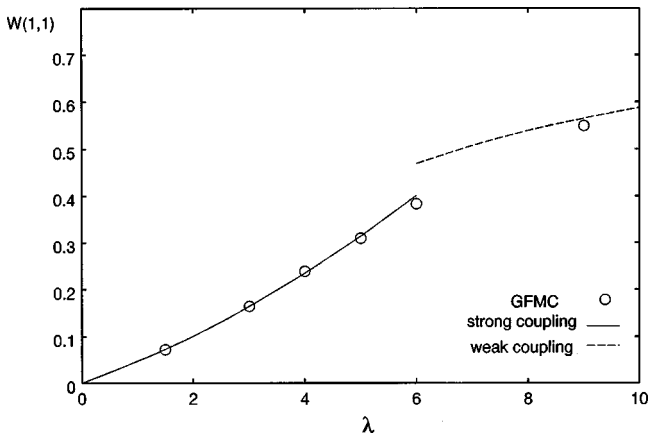

FIG. 8. The mean plaquette $W(1,1)$ for the bulk system graphed against coupling λ. The solid line represents the strong-coupling series expansion [19] and the dashed line the asymptotic weak-coupling behavior.

$$Ka^2 = \frac{aT}{c}, \tag{32}$$

where [26]

$$c \sim \frac{2}{g^2}[1-0.1671g^2] = \sqrt{\frac{2\lambda}{3}}\left[1-0.1671\sqrt{\frac{6}{\lambda}}\right], \quad \lambda\to\infty. \tag{33}$$

We have also used the weak-coupling relationship between the scales of Euclidean and Hamiltonian lattice Yang-Mills theory calculated by Hasenfratz and Hasenfratz [26] to plot the results against the Euclidean coupling $\beta=6/g_E^2$, where

$$\beta = \sqrt{6\lambda} - 0.01308. \tag{34}$$

It can be seen that the present GFMC results are in rough agreement with the axial string tension results in the region

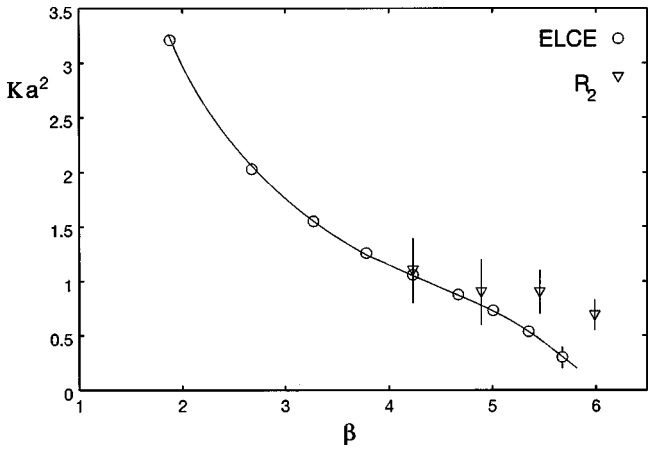

FIG. 9. The string tension Ka^2 graphed against coupling β. The circles are obtained from ELCE estimates of the axial string tension [19]; the triangles are Monte Carlo estimates of R_2.

$4 \leqslant \beta \leqslant 5$, which is also the region where the ''roughening'' transition occurs in the string tension [19]. For $\beta > 5$, however, the Creutz ratio R_2 runs above the ELCE estimate, and shows no sign of the expected crossover to an exponentially decreasing scaling behavior at $\beta \simeq 6$. We presume that this is a finite-size effect, and that the Creutz ratios R_n for larger n will show a substantial decrease in the ''weak-coupling'' regime $\beta \geqslant 6$. That is certainly the pattern seen in the Euclidean calculations [25] or in the $U(1)_{2+1}$ model [18]. Unfortunately, however, our present results for the larger Wilson loops are not of sufficient accuracy to allow worthwhile estimates of R_n for $n \geqslant 2$.

IV. SUMMARY AND CONCLUSIONS

We have presented the results of a new Green's function Monte Carlo study of the SU(3) Yang-Mills theory in the $(3+1)$D Hamiltonian formulation. A forward-walking method has been used to estimate values for the Wilson loops as well as the ground-state energy, and hence some rather crude estimates of the string tension have been extracted. Comparisons have been made with an earlier Hamiltonian calculation of the axial string tension [19]. The two sets of results agree in the ''roughening'' region, but our Monte Carlo results do not extend to the large Wilson loops that would be required to demonstrate ''scaling'' behavior in the weak-coupling regime.

Some significant problems with the GFMC method have emerged from this study. The ''forward-walking'' technique was introduced specifically to avoid any variational bias from the trial wave function [2,14–16]. As it turns out, however, the results for the Wilson loops show a substantial dependence on the trial wave function parameter c. The systematic error due to this dependence is an order of magnitude larger than the statistical error, so it would pay to put more effort in future studies into improving the trial wave function, rather than simply increasing the statistics [in this connection, we note that Beccaria [27] has recently proposed a ''stochastic reconfiguration'' method for dynamically optimizing the trial wave function in Hamiltonian LGT, and has applied it to the U(1) theory in $(2+1)$D and the SU(2) theory in $(3+1)$D]. Furthermore, the effective ensemble size decreases during each measurement as the descendants of each ''ancestor'' state die out, and this produces a substantial loss in statistical accuracy at weak coupling, as well.

It would be preferable if one were able to do away entirely with all the paraphernalia of trial wave function, weights, branching algorithms, etc., and just rely on some sort of Metropolis-style accept-reject algorithm to produce a correct distribution of walkers. Within a quantum Hamiltonian framework, a way is known to do this, namely the path integral Monte Carlo (PIMC) approach [20]. We conclude that the PIMC approach may be better suited than GFMC approach to the study of large and complicated lattice Hamiltonian systems.

ACKNOWLEDGMENTS

This work is supported by the Australian Research Council. Calculations were performed on the SGI Power Challenge Facility at the New South Wales Center for Parallel Computing and the Fujitsu VPP300 vector machine at the Australian National Universtiy Supercomputing Facility. We are grateful for the use of these facilities.

[1] J. Kogut and L. Susskind, Phys. Rev. D **11**, 395 (1975).
[2] D. M. Ceperley and M. H. Kalos, in *Monte Carlo Methods in Statistical Mechanics*, edited by K. Binder (Springer-Verlag, New York, 1979).
[3] S. A. Chin, J. W. Negele, and S. E. Koonin, Ann. Phys. (N.Y.) **157**, 140 (1984).
[4] R. Blankenbecler and R. L. Sugar, Phys. Rev. D **27**, 1304 (1983).
[5] T. A. DeGrand and J. Potvin, Phys. Rev. D **31**, 871 (1985).
[6] C. R. Allton, C. M. Yung, and C. J. Hamer, Phys. Rev. D **39**, 3772 (1989).
[7] C. J. Hamer, K. C. Wang, and P. F. Price, Phys. Rev. D **50**, 4693 (1994).
[8] D. Robson and D. M. Webber, Z. Phys. C **15**, 199 (1982).
[9] D. W. Heys and D. R. Stump, Phys. Rev. D **28**, 2067 (1983).
[10] D. W. Heys and D. R. Stump, Phys. Rev. D **30**, 1315 (1984).
[11] S. A. Chin, O. S. van Roosmalen, E. A. Umland, and S. E. Koonin, Phys. Rev. D **31**, 3201 (1985).
[12] S. A. Chin, C. Long, and D. Robson, Phys. Rev. Lett. **57**, 2779 (1986); **60**, 1467 (1988); C. Long, D. Robson, and S. A. Chin, Phys. Rev. D **37**, 3006 (1988); D. W. Heys and D. R. Stump, Nucl. Phys. **B257**, 19 (1985); **B285**, 13 (1987).
[13] S. A. Chin, C. Long, and D. Robson, Phys. Rev. D **37**, 3001 (1988).
[14] M. H. Kalos, J. Comput. Phys. **1**, 257 (1966).
[15] K. S. Liu, M. H. Kalos, and G. V. Chester, Phys. Rev. B **10**, 303 (1974).
[16] P. A. Whitlock, D. M. Ceperley, G. V. Chester, and M. H. Kalos, Phys. Rev. B **19**, 5598 (1979).
[17] M. Samaras and C. J. Hamer, Aust. J. Phys. **52**, 637 (1999).
[18] C. J. Hamer, R. J. Bursill, and M. Samaras, Phys. Rev. D **62**, 054511 (2000).
[19] C. J. Hamer, A. C. Irving, and T. E. Preece, Nucl. Phys. **B270**, 553 (1986).
[20] D. M. Ceperley, Rev. Mod. Phys. **67**, 279 (1995).
[21] M. A. Beg and J. Ruegg, J. Math. Phys. **6**, 677 (1965).
[22] K. J. Runge, Phys. Rev. B **45**, 7229 (1992).
[23] C. J. Hamer and Zheng Weihong, Phys. Rev. D **48**, 4435 (1993).
[24] T. Höfsass and R. Horsley, Phys. Lett. **123B**, 65 (1983).
[25] M. Creutz, *Quarks, Gluons and Lattices* (Cambridge University Press, Cambridge, England, 1983).
[26] A. Hasenfratz and P. Hasenfratz, Nucl. Phys. **B193**, 210 (1981).
[27] M. Beccaria, Phys. Rev. D **62**, 034510 (2000).